

# Gamma-Ray Bursts and the Cosmic Star Formation Rate

Mark Krumholz<sup>1</sup> and S. E. Thorsett<sup>2</sup>

Joseph Henry Laboratories and Department of Physics, Princeton University,  
Princeton, NJ 08544

and

Fiona A. Harrison<sup>3</sup>

Space Radiation Laboratory and Division of Physics, Mathematics and Astronomy,  
California Institute of Technology, Pasadena, CA 91125

Received \_\_\_\_\_; accepted \_\_\_\_\_

---

<sup>1</sup>krumholz@pulsar.princeton.edu

<sup>2</sup>Alfred P. Sloan Research Fellow; steve@pulsar.princeton.edu

<sup>3</sup>fiona@srl.caltech.edu

## ABSTRACT

We have tested several models of GRB luminosity and redshift distribution functions for compatibility with the BATSE 4B number versus peak flux relation. Our results disagree with recent claims that current GRB observations can be used to strongly constrain the cosmic star formation history. Instead, we find that relaxing the assumption that GRBs are standard candles renders a very broad range of models consistent with the BATSE number-flux relation. We explicitly construct two sample distributions, one tracing the star formation history and one with a constant comoving density. We show that both distributions are compatible with the observed fluxes and redshifts of the bursts GRB970508, GRB971214, and GRB980703, and we discuss the measurements required to distinguish the two models.

*Subject headings:* cosmology:observations – gamma rays:bursts – stars:neutron

## 1. Introduction

The recent measurements of redshifted absorption lines in the optical counterpart associated with GRB970508 (Metzger *et al.* 1997), and emission lines from the galaxies associated with GRB971214 (Kulkarni *et al.* 1998) and GRB980703 (Djorgovski *et al.* 1998) have confirmed the cosmological origin of gamma ray bursts. Such measurements offer a new method of estimating the distance and luminosity distribution of GRBs. Determining the redshift distribution, in particular, is of enormous importance in distinguishing between GRB source models. Much attention has focused on models in which burst activity is tied to the massive star formation rate, either directly (e.g., the “failed supernova” models of Woosley 1993), or with a time delay (e.g., the in-spiraling neutron star model of Paczyński 1986). In such models, GRB activity should trace the cosmic star formation history (Madau 1997; Fall, Charlot, & Pei 1996).

Previous analyses have attempted to constrain the GRB distribution using the cumulative number versus peak flux,  $N(< S)$ , relation observed by the BATSE instrument (e.g. Rutledge, Hui, & Lewin 1995). By making additional assumptions about the GRB luminosity distribution (usually that bursts are “standard candles”), various authors have reached strong conclusions about the GRB distribution. For example, Totani (1998) recently used GRB observations to argue that our understanding of the cosmic star formation rate is incorrect.

As we show in §3, relaxing the constraints on the intrinsic GRB luminosity function greatly reduces the power of GRB number counts to constrain the burst distribution. Standard candle models are no longer tenable; there are now redshift measurements of three bursts that vary in intrinsic luminosity by a factor of 20.<sup>1</sup> We demonstrate that a wide range of burst distributions are allowed by the current data, including both the BATSE measurements and the measured burst redshifts. However, we show in §4 that further redshift measurements, as well as deeper number counts, can be used to “deconvolve” the unknown redshift and luminosity distributions.

## 2. Theory

### 2.1. Tests Using Number Versus Flux

A source at redshift  $z$  has an integrated comoving luminosity in the bandpass  $[\nu_1, \nu_2]$  at the source given by  $L = \int_{\nu_1}^{\nu_2} \frac{dL}{d\nu} d\nu$ , where  $dL/d\nu$  is the spectrum of the source. If we assume a spectral form  $dL/d\nu = C\nu^{-\alpha}$ , we can compute the luminosity  $L'$  at Earth in the

---

<sup>1</sup>Unless otherwise stated, all models assume an  $H_0 = 75 \text{ km s}^{-1} \text{ Mpc}^{-1}$ ,  $\Omega_0 = 1.0$ ,  $\Lambda = 0$  cosmology, with no beaming.

bandpass  $[\nu'_1, \nu'_2]$ , where  $\nu' = \nu/(1+z)$ , using

$$L' = \frac{1}{1+z} \int_{\nu'_1}^{\nu'_2} C\nu^{-\alpha} d\nu' = (1+z)^{-\alpha} \int_{\nu_1}^{\nu_2} C\nu^{-\alpha} d\nu = (1+z)^{-\alpha} \cdot L. \quad (1)$$

The additional factor of  $1+z$  in equation (1) comes from time dilation at the burst source. The flux from the source observed at Earth is (Rutledge, Hui, & Lewin 1995)

$$S(z, L) = \frac{L(1+z)^{-\alpha}}{4\pi R_0^2 r(z)^2}. \quad (2)$$

The coordinate distance,  $r(z)$ , is given by Weinberg (1972)

$$r(z) = \frac{zq_0 + (q_0 - 1) (\sqrt{2q_0z + 1} - 1)}{H_0 R_0 q_0^2 (1+z)}. \quad (3)$$

Here  $R_0$ ,  $H_0$ , and  $q_0$  are the present-epoch expansion, Hubble, and deceleration parameters.

A model for GRB sources consists of a distribution in comoving redshift space,  $dp/dz$ , and a distribution in luminosity space,  $dg/dL$ . The redshift distribution has three parts: a geometric factor that accounts for the differential volume available at redshift  $z$ , a factor to include relativistic effects, and a factor  $n(z)$  for the comoving differential density of GRBs per unit volume at redshift  $z$ . Thus,  $dp/dz$  is given by

$$\frac{dp}{dz} = \frac{dV}{dz} \frac{1}{1+z} n(z) = 4\pi \frac{r(z)^2}{\sqrt{1 - kr(z)^2}} \frac{dr(z)}{dz} \frac{n(z)}{1+z}. \quad (4)$$

Here,  $dV/dz$  is the comoving volume element per unit redshift, the factor  $1/(1+z)$  comes from time dilation at the burst source, and  $k$  is  $-1$ ,  $0$ , or  $1$  for open, flat, and closed cosmologies, respectively.

To test a model, we generate a large number of bursts. We select redshifts from the distribution  $dp/dz$ , and luminosities from  $dg/dL$ . Using equation (2), we determine the flux for each burst in the sample, correct for flux-dependent instrumental sensitivity, and form a cumulative distribution function  $N(< S)$ . We compare the distribution function for the model to the observed  $N(< S)$  relation using a Kolmogorov-Smirnov (KS) test, calculating a confidence level at which that model can be ruled out.

## 2.2. Tests Using Redshift Measurements

With redshift measurements, we can compare a model's predicted redshift distribution to the observed distribution. It is necessary to correct the predicted distribution for the bias introduced by a finite flux cutoff. To do this, we generate a large number of bursts from the model, correct the sample for instrumental sensitivity, and simultaneously compare the redshift and flux distributions using a two-sided, two-dimensional KS test (Press *et al.* 1992).

### 3. Maps of Parameter Space

We examine range-dominated power law luminosity distributions, which have previously been studied by Emslie & Horack (1994) , Hakkila *et al.* (1996) , Horack *et al.* (1996) , Horváth *et al.* (1996) , and Loredó & Wasserman (1998) . These distributions have the form  $dg/dL = L^p$  in the range  $[L_{\min}, L_{\max}]$  and are zero everywhere else. For the star formation rate, we use the closed-box model of 280 nm cosmic emissivity, including dust obscuration, taken from Fall *et al.* (1996). This paper and others (e.g. Madau 1997) include several other estimates of the cosmic star formation history. We choose this model as an example; other SFR models would give numerically different but qualitatively similar results.

First, we find the comoving luminosity of the three GRBs in the BATSE bandpass (50-300 keV). GRB971214 has a peak flux of 1.9538 photons  $\text{cm}^{-2} \text{s}^{-1}$  on the 1024 ms time-scale, and a measured redshift of 3.42 (Kulkarni *et al.* 1998). GRB970508 has a peak flux of 0.969 photons  $\text{cm}^{-2} \text{s}^{-1}$ , absorption features at  $z = 0.835$  (Metzger *et al.* 1997), and it most likely in a galaxy at that distance (Pian *et al.* 1998). GRB980703 has a peak flux of 2.42 photons  $\text{cm}^{-2} \text{s}^{-1}$ , and is associated with an object at  $z = 0.967$  (Djorgovski *et al.* 1998). We obtained the BATSE peak fluxes from Meegan *et al.* (1998) .

To use equation (2), we need to know  $\alpha$ , the GRB spectral index. GRB spectra vary considerably (Band *et al.* 1993); a thorough treatment would assume a distribution of underlying spectra in its analysis. However, as we will see, the current data do not yet justify this expansion of the model phase space. Instead, we simplify by using as our single spectral index the recent estimate  $\alpha = 1.1$  (Mallozzi, Pendleton, & Paciesas 1996). With this assumption, we calculate luminosity  $L_1 = 2.15 \times 10^{50}$  erg/s for GRB970508,  $L_2 = 4.60 \times 10^{51}$  erg/s for GRB971214, and  $L_3 = 6.70 \times 10^{50}$  erg/s for GRB980703.

We examine the section of parameter space  $L_1/10 < L_{\min} < L_1$ ,  $L_2 < L_{\max} < L_2 \cdot 10$ ,  $-1 < p < -2.5$ , on a 21 by 21 by 11 grid evenly spaced in the logarithm of  $L_{\min}$  and  $L_{\max}$ , and evenly spaced in  $p$ .

The BATSE GRB catalog (Meegan *et al.* 1998), as of late July, includes 2195 bursts. To insure uniform efficiency, we restrict our study to the 1277 bursts triggered on channels 2+3 with a threshold of 5.5 sigma on all three BATSE time scales. We eliminate from this list 307 GRBs with peak flux below 0.42 photons  $\text{cm}^{-2} \text{s}^{-1}$ , where BATSE's efficiency is near unity. Efficiency drops rapidly below this cutoff, and uncertainties in efficiency contribute significantly to estimated number counts (Pendleton, Hakkila, & Meegan 1998). Using a KS test, we compare the remaining 970 bursts to 5000 GRBs generated from each model.

The resulting confidence levels are shown in Figure 1. The data clearly show there are a number of luminosity distributions consistent with a redshift distribution that goes as the star formation history. Our results are consistent with previous work indicating that the BATSE data constrain most GRBs to a single decade in luminosity (Horack *et al.* 1996). Despite this constraint, the BATSE data presently allow a very wide range of possibilities.

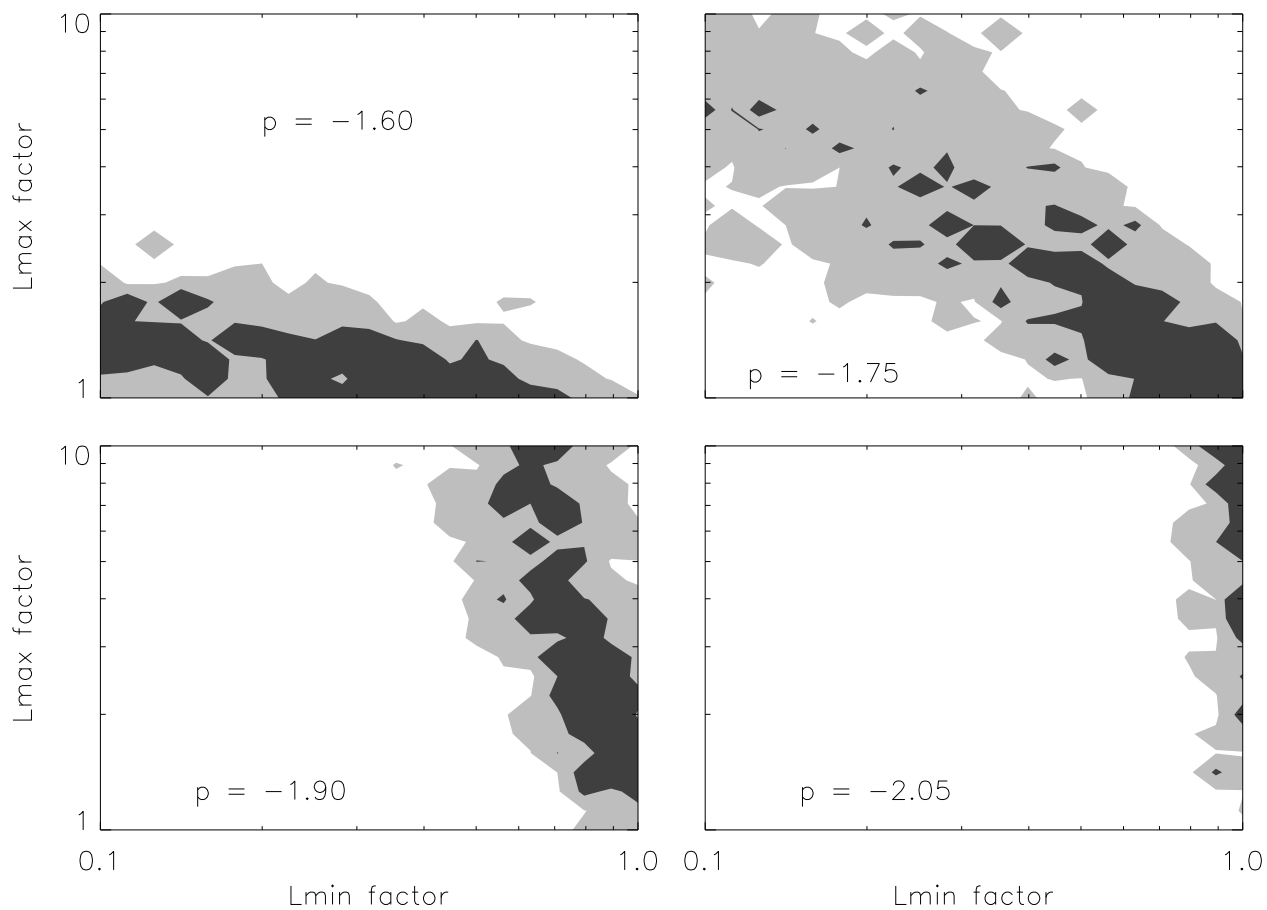


Fig. 1.— The light contour shows models with significance greater than 0.05, and the dark contour shows models with significance greater than 0.33. One minus the significance value is the confidence level at which the model can be ruled out.  $L_{\min}$  factor and  $L_{\max}$  factor indicate the amount by which the luminosities of GRB970508 and GRB971214 are multiplied, respectively. Values of  $p$ , the exponent of the luminosity distribution, are indicated in each panel.

#### 4. Case Study of Two Models

To determine what measurements can differentiate the models, we study two models, which we call the star formation rate model (SFR) and the constant comoving density model (CCD). SFR uses the star formation rate as its redshift distribution, and has  $L_{\min} = 1.52 \times 10^{50}$  erg/s,  $L_{\max} = 1.16 \times 10^{52}$  erg/s,  $p = -1.9$  for its luminosity distribution. The CCD model has a constant comoving redshift distribution, an  $L_{\min} = 1.13 \times 10^{50}$  erg/s,  $L_{\max} = 1.14 \times 10^{52}$  erg/s,  $p = -2.30$  for its luminosity distribution. Both these models fit the BATSE data with a KS significance higher than 0.33, and are also reasonably consistent with GRB970508, GRB971214, and GRB980703. Figure 2 shows where these three GRBs lie in comparison to the SFR model.

We test whether number versus flux measurements from an instrument more sensitive than BATSE can differentiate the models. We consider an instrument with a flux cutoff of  $0.06$  photons  $\text{cm}^{-2} \text{s}^{-1}$ , and perfect efficiency above this cutoff. Figure 2 shows that, while by construction the models predict identical numbers of bursts below the BATSE cutoff, they differ substantially at lower peak fluxes. Thus, the observed number of bursts per year can differentiate the models. As an interesting side note, in the SFR model, 48 percent of all GRBs in BATSE’s field of view are seen with a flux cutoff of  $0.42$  photons  $\text{cm}^{-2} \text{s}^{-1}$ , and 98 percent are above  $0.06$  photons  $\text{cm}^{-2} \text{s}^{-1}$ .

We do a KS comparison of the CCD model to a variable number of GRBs chosen from the SFR distribution. Our results indicate that more sensitive instruments than BATSE may be able to differentiate our sample models using only the number-flux relation. One hundred and twenty-five bursts are enough for a two-sigma differentiation 95 percent of the time. The hypothetical instrument could make this observation in about 4 months, assuming 50 percent sky coverage and unit efficiency.

While these results are encouraging, it seems unlikely that observations of flux alone would do this well in all cases. Based on  $N(< S)$ , one model with many bright GRBs at high redshift might well be completely indistinguishable from another with dim GRBs at low redshift. In this case, redshift determinations would be necessary to differentiate the models.

As shown in Figure 2, the two models predict substantially different redshift distributions for the bursts. In order to determine the number of redshift measurements required to distinguish the two models, using BATSE’s efficiency, we compared the CCD model to a variable number of bursts from the SFR distribution in a two-sided, two-dimensional KS test on the peak fluxes and redshifts.

Our results indicate that about 25 redshifts are needed to distinguish the SFR and CCD models at the two sigma level 95 percent of the time. Our method is, however, a significant oversimplification: we assume that it is equally easy to measure any redshift. In practice, different measurement techniques result in an efficiency with strong and

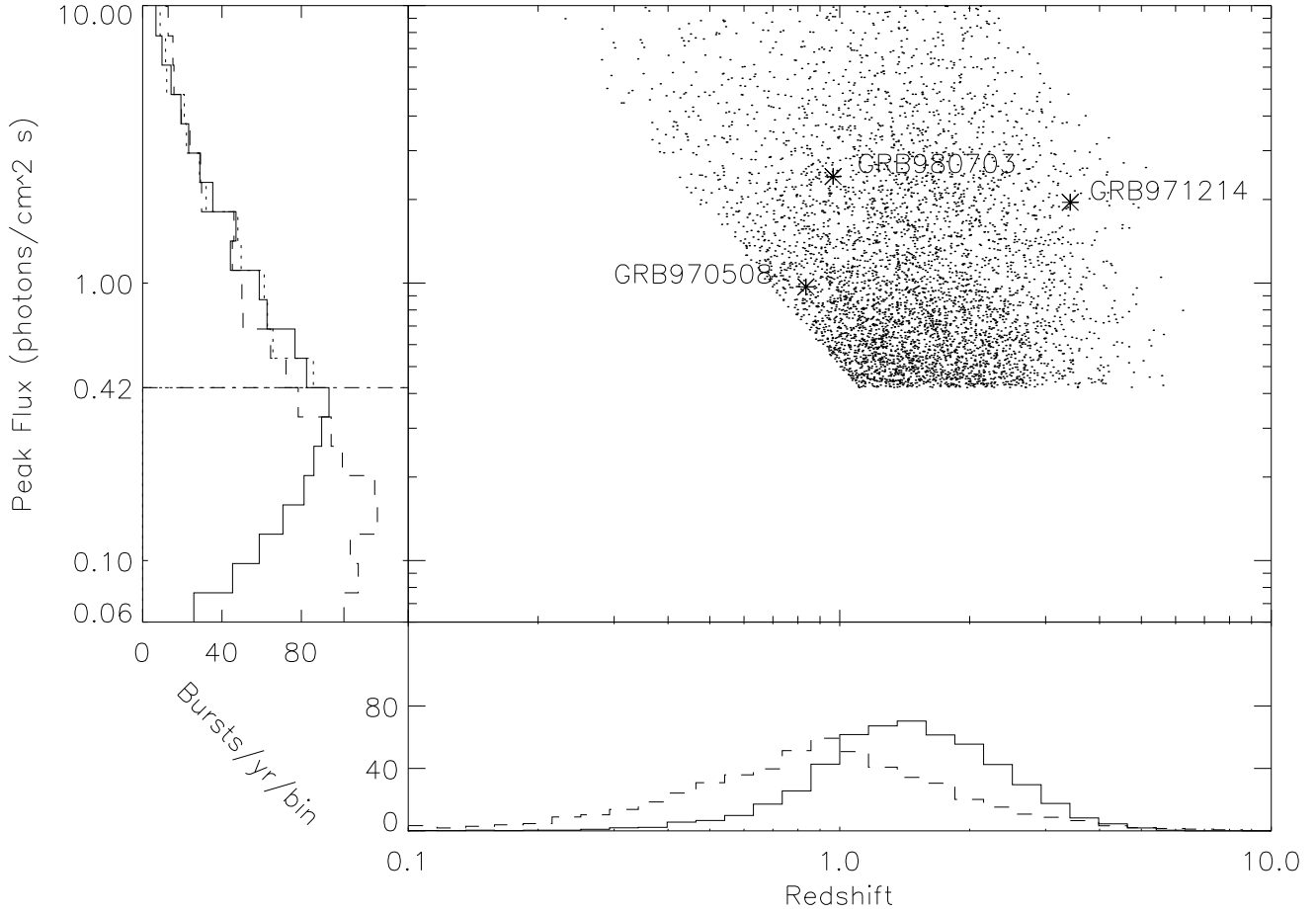


Fig. 2.— The center panel shows points indicating the peak flux and redshift for 5000 GRBs selected from the SFR distribution with the BATSE flux cutoff; the asterisks are GRB970508, GRB971214, and GRB980703. The left panel shows the number of GRBs per year in each peak flux range, divided into 20 evenly spaced logarithmic bins. The dot-dash vertical line shows the BATSE flux cutoff. The histogram in the bottom panel shows the expected number of bursts per year in each redshift range, divided into 30 evenly spaced logarithmic bins. The total number of bursts is generated by setting the number in each model equal to the number per year seen by BATSE, corrected for BATSE’s effective coverage of 48.3 percent of the sky. In left and bottom panels, the solid histogram is the SFR model, and the dashed histogram is the CCD model. The dotted line in the left panel is the BATSE catalog.



complicated redshift dependence, with redshifts between  $\sim 1$  and 2, where the bulk of star formation occurs, difficult to measure from the ground.

Furthermore, two-dimensional KS tests are somewhat unreliable with small numbers of data points (Press *et al.* 1992). Parameters for the two-dimensional KS test are derived by numerical experiment, and assume that the number of samples is large enough for statistical treatment. Samples with fewer than about 20 data points give results that depend on the shape of the underlying distribution. Thus, our figures should be regarded only as lower bounds. Even so, we note that there are three measured redshifts out of fifteen accurate localizations. Given this efficiency, we would need more than 125 localizations to reach even this lower limit.

## 5. Conclusion

Our results indicate that the current data available from BATSE are insufficient to determine the redshift distribution of GRBs. The complicated mixing between luminosity and comoving redshift distributions make it impossible to significantly constrain either one at present. Our example models demonstrate that even a relatively small change in luminosity distribution can render both a star formation model and a constant comoving density model consistent with observations.

The increased flux sensitivity provided by the next generation of satellites should be able to greatly reduce the parameter space available. If our comparison of the SFR and the CCD model is representative, more sensitive satellites may be able to confirm whether GRBs trace the star formation history even without localizing any bursts. However, redshift measurements provide considerably stronger constraints on GRB models.

These results indicate that the best way to constrain the spatial distribution of GRBs is by directly measuring a sizable number of redshifts. As has been demonstrated by the Beppo-SAX localizations, this is best accomplished by rapid ground-based optical spectroscopic followup of accurately-positioned bursts, or optical spectroscopy of the host galaxies. A lower limit on the number of GRB localizations required to distinguish between disparate models, based on current efficiency, is more than a hundred. This is in excess of what will likely be achieved by continued operation of Beppo-SAX, and by the upcoming HETE-2 mission (which expects to localize  $< \sim 50$  bursts). It is likely, however, that more rapid notification to the ground of positions at the arc-minute or better level ( $\sim 8'$  SAX positions currently take 8 hours before distribution, and refinement to  $1'$  typically requires a day) will increase the efficiency for redshift determination by absorption spectroscopy of the optical afterglow. If this is the case, it is possible that the next generation of satellites may be able to test whether the spatial distribution of GRB sources follows star formation.

The authors wish to thank S. M. Fall, S. Charlot, and Y. C. Pei for their data on the cosmic star formation history, David Hogg for useful discussions, and the referee for helpful comments on the manuscript. This work is partially supported by a grant from the National Science Foundation.

## REFERENCES

- Band, D. *et al.* 1993, ApJ, 413, 281
- Djorgovski, S. G. *et al.* 1998, GCN notice 139
- Emslie, G. A. & Horack, J. M. 1994, ApJ, 435, 16
- Fall, S. M., Charlot, S., & Pei, Y. C. 1996, ApJ, 464, L43
- Hakkila, J. *et al.* 1996, ApJ, 462, 125
- Horack, J. M., Hakkila, J., Emslie, A. G., & Meedgan, C. A. 1996, ApJ, 462, 131
- Horváth, I., Mészáros, P., & Mészáros, A. 1996, ApJ, 470, 56
- Kippen, R. M. *et al.* 1997. IAU circular 6789
- Kippen, R. M. *et al.* 1998, GCN notice 143
- Kulkarni, S. R. *et al.* 1998, Nature, 393, 35
- Loredo, T. J. & Wasserman, I. M. 1998, ApJ, 502, 75
- Madau, P. 1997. IAU circular 186
- Mallozzi, R. S., Pendleton, G. N., & Paciesas, W. S. 1996, ApJ, 471, 636
- Meegan, C. A. *et al.* 1998, Available at <http://www.batse.msfc.nasa.gov/data/grb/catalog>
- Metzger, M. R., Djorgovski, S. G., Kulkarni, S. R., Steidel, C. C., Adelberger, K. L., Frail, D. A., Costa, E., & Fronterra, F. 1997, Nature, 387, 879
- Paczynski, B. 1986, ApJ, 308, L43
- Pendleton, G. N., Hakkila, J., & Meegan, C. A. 1998, in 4th Huntsville Gamma-Ray Burst Symposium, ed. C. A. Meegan, R. Preece, & T. Koshut, (Woodbury, New York: AIP), 899
- Pian, E. *et al.* 1998, ApJ, 492, L103
- Press, W. H., Teukolsky, S. A., Vetterling, W. T., & Flannery, B. P. 1992, Numerical Recipes: The Art of Scientific Computing, 2<sup>nd</sup> edition, (Cambridge: Cambridge University Press)
- Rutledge, R. E., Hui, L., & Lewin, W. H. G. 1995, MNRAS, 276, 753
- Totani, T. 1998, preprint, astro-ph/9805263

Weinberg, S. 1972, *Gravitation and Cosmology: Principles and Applications of the General Theory of Relativity*, (New York: Wiley)

Woosley, S. E. 1993, *ApJ*, 405, 273